PHYSICAL REVIEW C VOLUME 36, NUMBER 4 OCTOBER 1987

Coulomb and nuclear excitation of giant dipole resonances in (α,α') inelastic scattering

S. Shlomo
Center for Theoretical Physics, Department of Physics, and Cyclotron Institute, Texas A&M University, College Station, Texas 77843

Y. -W. Lui and D. H. Youngblood
Cyclotron Institute, Texas A&M University, College Station, Texas 77843

T. Udagawa and T. Tamura
Department of Physics, University of Texas, Austin, Texas 78712
(Received 22 January 1987)

Cross sections of inelastic α-particle scattering to isovector giant dipole resonances are calculated including both nuclear and Coulomb excitation. It is shown that the calculated cross sections are rather small and can be safely neglected for bombarding energies less than 200 MeV in determining the strength of the giant monopole resonance. This conclusion contradicts that of a recent report made by Peterson.

I. INTRODUCTION

As is well known, inelastic alpha scattering has been used successfully in identifying isoscalar giant monopole resonances (GMR).[1-4] Important nuclear structure information like the monopole strength and the nuclear compressibility were then extracted.

In order to extract this nuclear structure information from the experimental (α,α') data, however, theoretical calculations of these cross sections have to be done. In achieving these fits, it has been customary to consider only GMR contributions and to ignore the contributions from the excitation of the isovector giant dipole resonance (GDR). It has been previously argued[1,5] that the GDR contribution to the (α,α') cross section is rather small.

The calculation of the GDR cross section in Ref. 1 was done, however, by considering only the nuclear part of the excitation, while the calculation in Ref. 5 considered both nuclear and Coulomb parts of the excitation. Unfortunately, however, the relative sign of these two parts was taken erroneously in Ref. 5, and it is one of the major purposes of this paper to present new results, after this error is corrected. (The two parts should interfere constructively. In Ref. 5, they interfered destructively.) It will be seen below, nevertheless, that the major conclusions of Ref. 5 remain largely unchanged. In fact, except for the highest bombarding energies studied ($E_\alpha=218$ MeV), the GDR cross section remains small compared to the GMR cross section even when the nuclear and Coulomb parts interfere constructively. The GDR cross section with constructive interference does become important for higher energy α particles.

Recently Peterson[6] reported distorted-wave Born approximation (DWBA) calculations that gave a GDR cross section sufficiently large to reproduce the experimental (α,α') cross section attributed to the GMR in Ref. 1. In light of the results reported in this paper, we believe that Peterson's conclusion is not valid. A short paper discussing Peterson's work has been submitted for publication recently.[7]

Unfortunately, the details of Peterson's calculation are not available to us. Further, he provided no discussion comparing his calculations to our previous GDR calculations of Refs. 1 and 5, so from his report all of the reasons for the disagreement were not *a priori* obvious. We point out later that Peterson's result is mainly due to a coupling potential (nuclear plus Coulomb) which is too large. We also note that some other previous calculations[4] were carried out using a destructive interference between the nuclear and the Coulomb parts, leading to lower cross sections for the isovector giant dipole state. This can be seen from the expression for the coupling potential and the results shown in the figures of Ref. 4. We stress that the nuclear and the Coulomb coupling potentials should interfere constructively for isovector states and destructively for isoscalar states. Having these facts in mind and considering the importance of proper theoretical calculations for extraction of the experimental parameters, we decided to present in this paper the formulation of the GDR cross section in detail. In doing this, we also give our formalism an added flexibility so that we can discuss the GDR cross section on a basis which is much broader than what was presented in Ref. 5. In other words, what we intend to do in this paper is both to correct the error in Ref. 5 and to go much beyond what was presented in Ref. 5 to provide a comprehensive description for future work.

In what follows, we discuss in Sec. II the method of the calculation, particularly the construction of the coupling potentials that we use in the present calculation. In Sec. III, we present the results of numerical calculations. The final remarks of the present work are given in Sec. IV, where we also discuss the work by Peterson.[6]

II. METHOD OF CALCULATIONS

A. Cross section formula

In this work, we carried out coupled-channel (CC) calculations of the GDR and GMR cross sections, including Coulomb excitation as well as nuclear excitation. We used for this purpose the computer code JPWKB developed some time ago by Kim *et al.*[8] This code allows us to perform fast and accurate calculation of the Coulomb excitation cross section. Since the details of the calculation were described in Refs. 5 and 8, we give here only the basic idea.

The CC equations are solved exactly up to a certain radius $r=R_s$, which is somewhat larger than the classical turning point. For this purpose, we use the program JUPITER-1.[8,9] The CC equations for $r>R_s$ are, however, solved approximately by using a WKB-type approximation originally introduced by Alder and Pauli.[10] Once the CC equations are solved in this way, one can obtain the S matrix. The cross section can then be calculated as

$$\frac{d\sigma}{d\Omega}=\frac{1}{2I_0+1}\sum_{M_0M_n}|X_{M_nM_0}|^2 , \tag{1a}$$

where

$$X_{M_nM_0}=\frac{i}{2}\sum_{ll'}\frac{4\pi}{(kk')^{1/2}}e^{i(\sigma_l+\sigma_{l'})}\langle lI_00M_0\,|\,JM_0\rangle\langle l'I_nm_{l'}M_n\,|\,JM_0\rangle S^J_{l'I_n,lI_0}Y_{l'm_{l'}} . \tag{1b}$$

In (1), I_0M_0 and I_nM_n are the spin and its projection of the initial and final states, k is the wave number, and σ_l is the Coulomb phase shift for the partial wave l. The unprimed and primed quantities are for the incident and exit channels, respectively.

The most critical quantities that enter into the calculation are the coupling potentials. In the rest of this section, we shall thus concentrate on them. We derive them for both GDR and GMR excitations.

B. Coupling potential for GDR excitation

In deriving the coupling potential, we adopt the Goldhaber-Teller model for the GDR and follow (as is also done in Ref. 5) basically the prescription of Satchler.[11] In Ref. 11, however, it was assumed that the central densities of the proton and neutron distributions were the same. In the present study, we remove this restriction and treat the densities in a somewhat more general way. More precisely, we introduce the parameter α which is related to the ratio of the central densities of the proton and neutron distributions by

$$\rho_p(r=0)/\rho_n(r=0)=\frac{Z+\alpha(N-Z)/2}{N-\alpha(N-Z)/2} . \tag{2}$$

The parameter α, deduced from experiment, plays an important role in the work of this paper. $\rho_i(r)$ with $i=$p ($i=$n) is the proton (neutron) density, and Z and N are the proton and neutron numbers of the target. A new parameter δ which is related to the radii, R_i, of the proton and neutron density distributions, is then introduced by

$$\delta=(R_n-R_p)/2 . \tag{3}$$

By imposing the condition that the integral of ρ_n and ρ_p over the nuclear volume is equal to N and Z, respectively, we obtained, to first order in $\alpha(N-Z)/A$, that δ is given by

$$\delta=\alpha\frac{1}{3}\frac{N-Z}{A}R_0 , \tag{4}$$

with

$$R_0=(R_n+R_p)/2 . \tag{5}$$

It is seen from (4) that the parameter δ can be used interchangeably with α.

We point out that in the extreme cases of $\alpha=0$ and 1, we have

$$\alpha=0,\quad R_n=R_p,\quad N\rho_p(0)=Z\rho_n(0) \tag{6a}$$

$$\alpha=1,\quad R_n-R_p=\frac{2}{3}\frac{N-Z}{A}R_0,\quad \rho_p(0)=\rho_n(0) . \tag{6b}$$

Equation (6b) describes the assumption made in Ref. 11 of equal central densities.

In order to derive the coupling potential, we again follow Ref. 11. Let us assume that the center of mass of the neutrons and protons are displaced, respectively, by $(Z/A)\mathbf{d}$ and $(-N/A)\mathbf{d}$ from the center of mass of the nucleus. Clearly, $\mathbf{d}$ is a coordinate vector that describes the dipole oscillations. The proton and neutron densities $\rho_i(r)$ ($i=$p and n) are then varied as

$$\begin{aligned}\rho_i(r)&\rightarrow\rho_i(\,|\,\mathbf{r}+g_i\mathbf{d}\,|\,)\\&\simeq\rho_i(r)+\left[\frac{4\pi}{3}\right]^{1/2}g_i\frac{\partial\rho_i}{\partial r}\Sigma_M d^*_M Y_{1M} ,\end{aligned} \tag{7}$$

where $g_p=N/A$ and $g_n=-Z/A$, and d_M (and d^*_M) stands for the spherical components (and its conjugate) of the displacement vector $\mathbf{d}$. Y_{1M} are the spherical harmonics. We remark here that the dipole oscillations described by the above displacements of the centers of mass of the proton and neutron density distributions satisfy the requirement that the center of mass position of the whole nucleus is kept fixed.

The coupling potential ΔU can be deduced from (7) by invoking the assumption that the deformation of the optical potential follows that of the density. However, to make our discussion more transparent, we adopt the folding model for constructing ΔU. The coupling potential is then obtained by folding the transition density,

$$\rho_{\rm tr}(r)=\left[\frac{4\pi}{3}\right]^{1/2} g_i \frac{\partial\rho_i}{\partial r}\Sigma_M d_M^* Y_{1M} \ , \tag{8}$$

taken from (7), with the two-body interaction $v(\mathbf{r},\mathbf{r}')$. We thus have

$$\Delta U=\mathrm{Tr}\int \rho_{\rm tr}(\mathbf{r}')v(\mathbf{r},\mathbf{r}')d\mathbf{r}'+(\text{exchange}) \ . \tag{9}$$

For completeness of the formulation, we first construct ΔU for a nucleon probe. The required ΔU for the α-particle probe is then obtained by adding the contributions of the neutrons and protons in the α particle. The nucleon-nucleon two-body interaction is given as

$$v(\mathbf{r},\mathbf{r}')=v_0(\mathbf{r},\mathbf{r}')+v_1(\mathbf{r},\mathbf{r}')\boldsymbol{\tau}\cdot\boldsymbol{\tau}' +\tfrac{1}{4}(1-\tau_3)(1-\tau_3')\frac{e^2}{|\mathbf{r}-\mathbf{r}'|} \ . \tag{10}$$

Note that the real part of the isoscalar v_0 (isovector v_1) interaction is negative (positive). Substituting (10) in (9) one finds for a *proton* projectile that

$$\Delta U^{\rm p}=\Delta U_N+\Delta U_C \ , \tag{11}$$

where the nuclear part of the coupling potential is given by

$$\Delta U_N=\left[\left[\frac{N}{A}\frac{\partial U_{0\rm p}}{\partial r}-\frac{Z}{A}\frac{\partial U_{0\rm n}}{\partial r}\right] +\left[\frac{N}{A}\frac{\partial U_{1\rm p}}{\partial r}+\frac{Z}{A}\frac{\partial U_{1\rm n}}{\partial r}\right]\right]\left[\frac{4\pi}{3}\right]^{1/2}\Sigma_M d_M^* Y_{1M} \ , \tag{12}$$

and the Coulomb part has the form

$$\Delta U_C=\left[\frac{4\pi}{3}\right]^{1/2}\frac{N}{A}F_C(r)\Sigma_M d_M^* Y_{1M} \ , \tag{13}$$

with

$$F_C(r)=-\frac{zZe^2}{r^2}\left[\theta(r-R_c)+\theta(R_C-r)\frac{r^3}{R_C^3}\right] \ . \tag{14}$$

In (12) $U_{0\rm p}$ ($U_{1\rm p}$) and $U_{0\rm n}$ ($U_{1\rm n}$) are the isoscalar (isovector) optical potentials due to the target protons and neutrons, respectively. They are obtained from

$$\begin{aligned} U_{0i}&=\int \rho_i(\mathbf{r}')v_0(\mathbf{r},\mathbf{r}')d\mathbf{r}' \ , \\ U_{1i}&=\int \rho_i(\mathbf{r}')v_1(\mathbf{r},\mathbf{r}')d\mathbf{r}' \ . \end{aligned} \tag{15}$$

The step function $\theta(x)$ in (14) is defined by $\theta(x)=1$ for $x>0$ and $\theta(x)=0$ for $x<1$, R_C is the Coulomb radius, and z is the projectile charge ($z=1$ for a proton and $z=0$ for a neutron).

For a neutron projectile, the coupling potential is obtained from (12) with opposite sign for the second term in (12) (with U_{1i}). Therefore, for an isospin $t=0$ projectile, such as a deuteron or α particle, only the term with U_{0i} contributes to ΔU. For the Coulomb part we have $z=1$ and 2 for a deuteron and α particle, respectively. It should be pointed out that, due to the conservation of the center of mass, the term with U_{0i} in (12) vanishes when $R_{\rm n}=R_{\rm p}$, i.e., in the case of (6a).

We now expand ρ_i as a Tayler series of δ. Retaining only the lowest order term, they can be obtained as

$$\rho_i=\left[\tfrac{1}{2}+\tau_i(1-\alpha)\frac{N-Z}{2A}\right]\rho_0-\tau_i\frac{R_0}{6}\alpha\frac{N-Z}{A}\frac{\partial\rho_0}{\partial r} \ , \tag{16}$$

where $\tau_{\rm n}=1$ and $\tau_{\rm p}=-1$, and

$$\rho_0=\rho_{\rm n}(\alpha=0)+\rho_{\rm p}(\alpha=0) \ . \tag{17}$$

[Note that ρ_i defined by (16) satisfies the condition that $\rho_{\rm p}+\rho_{\rm n}=\rho_0$ for any value of α.] Inserting (16) into (8), and substituting in (9), one finds using (10) that the coupling potential for a *proton* projectile is given by

$$\Delta U=\left[\frac{4\pi}{3}\right]^{1/2}\left[\tfrac{1}{2}[F_N(r)+F_N^1(r)]+\frac{N}{A}F_C(r)\right]\Sigma_M d_M^* Y_{1M} , \tag{18}$$

where $F_C(r)$ is given by (14) and

$$F_N(r)=\alpha\frac{N-Z}{A}\left[\frac{\partial U_0}{\partial r}+\frac{R_0}{3}\frac{\partial^2 U_0}{\partial r^2}\right] , \tag{19}$$

$$F_N^1(r)=\left[1-\left[\frac{N-Z}{A}\right]^2\right]\frac{\partial U_1}{\partial r} +\alpha\left[\frac{N-Z}{A}\right]^2\left[\frac{\partial U_1}{\partial r}+\alpha\frac{R_0^1}{3}\frac{\partial^2 U_1}{\partial r^2}\right] . \tag{20}$$

Here, $U_0<0$ ($U_1>0$) is the isoscalar (isovector) part of the proton's optical potential, obtained by folding the mass density ρ_0 with the isoscalar (isovector) interaction $v_0(v_1)$ of (10). The radii R_0 and R_0^1 are now those of the potentials U_0 and U_1, respectively.

We now write d_M^* as

$$d_M^*=d_0[c_{1M}^\dagger+(-1)^{1+M}c_{1-M}] \ , \tag{21}$$

where $c_{1M}^\dagger$ (c_{1M}) is the creation (annihilation) operator of the GDR phonon, while d_0 is the amplitude of the zero point oscillation. This d_0 can be related to the energy of the GDR phonon, E_x, and the mass parameter $\mu=(NZ/A)m$ (m is the nucleon mass) as

$$d_0=(\hbar^2/2\mu E_x)^{1/2}=(A\hbar^2/2NZmE_x)^{1/2} \ . \tag{22}$$

Inserting (21) with (22) into (18) we get that

$$\Delta U^{\rm p}=[\beta_N R_0 F_N(r)+\beta_N^1 R_0^1 F_N^1(r)+\beta_C R_C F_C(r)](1/3)^{1/2} \times\Sigma_M[c_{1M}^\dagger+(-1)^{1+M}c_{1-M}]Y_{1M} \ , \tag{23}$$

for the *proton* projectile. Here we have

$$\beta_N R_0=\beta_N^1 R_0^1=\frac{A}{2N}\beta_C R_C \ , \tag{24}$$

$$\beta_C=\left[\frac{4\pi N}{AZ}\frac{\hbar^2}{2mR_C^2E_x}\right]^{1/2} . \tag{25}$$

As indicated earlier, the corresponding coupling po-

tential for a neutron projectile is given by (23) with $F_C \equiv 0$ and the second term (with $F_N^{\dagger}$) is of the opposite sign. Therefore, by adding the contributions of the neutrons and protons in the α particle we get the final form for the coupling potential for the α-particle projectile. This coupling potential which is used in our calculations has the form

$$\Delta U^{\text{alpha}} = [\beta_N R_0 F_N(r) + \beta_C R_C F_C(r)](1/3)^{1/2} \times \Sigma_M [c^{\dagger}_{1M} + (-)^{1+M} c_{1-M}] Y_{1M} \ . \quad (26)$$

The first and second terms in (26) are, respectively, the nuclear and the Coulomb coupling terms. The nuclear form factor, F_N, is obtained from (19) with U_0 being the optical potential for the α particle, and the Coulomb form factor F_C is obtained from (14) with $z=2$. The values of β_N and β_C are given in (24) and (25).

Since δ is normally positive, $\alpha(N-Z)/A$ is also positive. From (25), it is seen that β_C is also positive. We now note that the nuclear form factor F_N given by (19) consists of two terms, i.e., of the first and second derivatives of the optical potential U_0. Since U_0 is negative with the decreasing magnitude as r increases, the first derivative is positive definite. On the other hand, the second derivative is positive for $r < R_0$, and is negative for $r > R_0$. Since the second derivative dominates (in magnitude) the first derivative at large r, F_N is positive up to a certain radius, say, $r = R_t$, and becomes negative for $r > R_t$. This R_t may be slightly larger than R_0. Since $F_C < 0$, as seen in (14), it is concluded that the sign of F_N is the same as that of F_C, once r exceeds R_t. In other words, the nuclear and Coulomb excitations interfere constructively at larger r. Since the α particle is strongly absorptive, the scattering takes place dominantly at large r, and the net interference is expected to be constructive. This is indeed the case, as will be shown in Sec. III.

As seen in (19), F_N is proportional to α. In Ref. 5, the value of α was taken to be -1. This choice of the sign of F_N was incorrect. Also, various information now available indicates that the (absolute) magnitude of α is much smaller than 1. In Table I, we have summarized recent information about the α value available at present. [These values were determined from the analyses of high energy proton[12] and pion[13] scattering and from Hartree-Fock (HF) calculations.[14]] The α values given in Table I are for the targets (^{90}Zr, ^{116}Sn, and ^{208}Pb) of the (α,α') scattering, which we are to analyze in Sec. III. The value of α is somewhat scattered, but is consistently smaller than 0.5. Note that the average value of α deduced from ground state densities is as small as 0.13. Continuum effects, related to single particle decay, may affect the transition density in a way to slightly increase the value of α. However, taking into account the long range random phase approximation (RPA) correlations, one finds only a small change in the value of α.[16,17] (See, for example, Fig. 1 of Ref. 17.) Taking these small effects into consideration, a value for α of 0.5 may be taken as the upper limit of α. The calculations described in Sec. III were done with several values of α. We stress that our conclusion does not change if we adopt the value of $\alpha = 1$.

TABLE I. Values of α for ^{90}Zr, ^{116}Sn, and ^{208}Pb. These values were taken from Table VII of Ref. 14.

Target	α_{expt}			α_{HF}
^{90}Zr	0.12	0.24 0.05	0.22	0.13
^{116}Sn	0.23			0.14
^{208}Pb	0.17	0.02	0.01 0.05	0.13

C. Coupling potential for GMR excitation

For the GMR cross section calculation, we used the coupling potential given in Ref. 15. We quote here only the final expression, which is

$$\Delta U = [\beta_N F_N(r) + \beta_C F_C(r)](c^{\dagger}_0 + c_0) Y_{00} \ , \quad (27)$$

where

$$F_N(r) = 3U_0 + r\frac{\partial U_0}{\partial r} \ , \quad (28)$$

$$F_C(r) = -\frac{zZe^2}{R_C^3}\tfrac{3}{2}(R_C^2 - r^2)\theta(R_C - r) \ , \quad (29)$$

and

$$\beta_N = \beta_C = \left[\frac{20\pi}{3}\frac{\hbar^2}{2mR_0^2 A}\frac{1}{E_x}\right]^{1/2} . \quad (30)$$

In the above, we included the Coulomb coupling term which interferes destructively with the nuclear coupling term. It is, however, unimportant for strongly absorptive projectiles since it is nonvanishing only for $r < R_C$.

III. NUMERICAL CALCULATIONS

The numerical calculations were performed by using the coupled-channel code JPWKB.[8] In the present calculations, we took into account radial distance up to 600 fm, and also partial waves up to 250. Our calculations are therefore very accurate down to a scattering angle of 1°, which is of particular importance for the GMR. In comparison, according to Peterson,[6] his DWBA calculation could be in error by as much as 50% at 5°. The coupling potentials of (26) and (27), with 100% of the corresponding energy weighted sum rule, were used in our calculations for the GDR and the GMR, respectively. The optical model potentials used in the calculations are summarized in Table II.

The calculated GDR cross sections (σ_D^{calc}) with $\alpha = 1.0$, 0.0, and -1.0 are presented in Figs. 1–3 by solid, dashed-dotted, and dashed lines, respectively. The dashed-dotted lines with $\alpha = 0.0$ are for pure Coulomb excitation as there is no nuclear contribution. The contribution due to the pure nuclear excitation, with $\alpha = 1$,

TABLE II. Optical potential parameters used in the calculation. These parameters were taken from Refs. 1–4.

Target	E_{lab} (MeV)	V (MeV)	r (fm)	a (fm)	W (MeV)	r_I (fm)	a_I (fm)	r_C (fm)
^{90}Zr	96	45.7	1.50	0.70	27.7	1.50	0.70	1.30
^{116}Sn	129	60.8	1.40	0.73	40.9	1.40	0.73	1.35
^{208}Pb	96	89.3	1.35	0.71	52.7	1.35	0.71	1.30
	129	89.3	1.35	0.71	52.7	1.35	0.71	1.30
	172	155.0	1.282	0.677	23.26	1.478	0.733	1.30
	218	119.9	1.26	0.74	21.3	1.45	0.80	1.30

are presented by the dotted lines in Figs. 1 and 2. It is seen that, as expected, the nuclear and Coulomb excitations interfere constructively for the case of $\alpha=1.0$, but destructively for the case of $\alpha=-1.0$. The destructive interference ($\alpha=-1.0$) is incorrect, but we present the results for the purpose of comparison with previous calculations.

At the lower incident energy, $E_\alpha=96$ MeV, σ_D^{calc} is dominated by nuclear excitation. As E_α increases, both contributions increase. Coulomb excitation, however, increases faster than does nuclear excitation, and at the highest energy considered ($E_\alpha=218$ MeV), the Coulomb excitation is larger (see Fig. 3).

Because of the constructive interference, σ_D^{calc} with $\alpha=1$ is larger than is σ_D^{calc} with $\alpha=0$, and σ_D^{calc} with $1>\alpha>0$ should lie between the two curves with $\alpha=0$ and 1. It should then be noted that σ_D^{calc}, even with $\alpha=1$ (which is twice the upper limit of 0.5 for a reasonable α value), is much smaller (for $E_\alpha=96$ MeV) than is σ^{expt}. Therefore, at this lower E_α, we may safely ignore the contribution from GDR in extracting the strength of GMR. However, σ_D^{calc} increases with increased E_α, and at the higher energies of $E_\alpha=178$ and 218 MeV, the σ_D^{calc} with $\alpha=1$ exceeds σ^{expt} at some angles where σ^{expt} is small. Except at these angles, however, σ_D^{calc} is still much smaller than σ^{expt}. In any case, for a more reasonable (smaller) α, σ_D^{calc} will be consistently smaller than σ^{expt}. It should also be noted that for $\alpha=1$, the angular distribution of σ_D^{calc} is consistently out of phase with σ^{expt}.

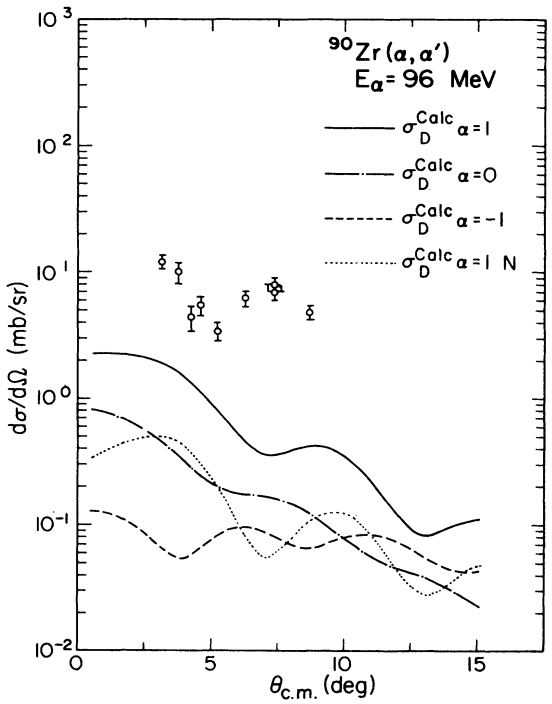

FIG. 1. Calculated GDR cross section for the ^{90}Zr(α,α') with $E_\alpha=96$ MeV, exhausting 100% of the energy weighted sum rule (solid curve). The dashed-dotted line is for pure Coulomb excitation and the dotted line is for pure nuclear excitation. Also shown, for comparison, the result for a destructive interference (dashed curve). The data are for the GMR with $E_x=16.2$ MeV, taken from Ref. 2.

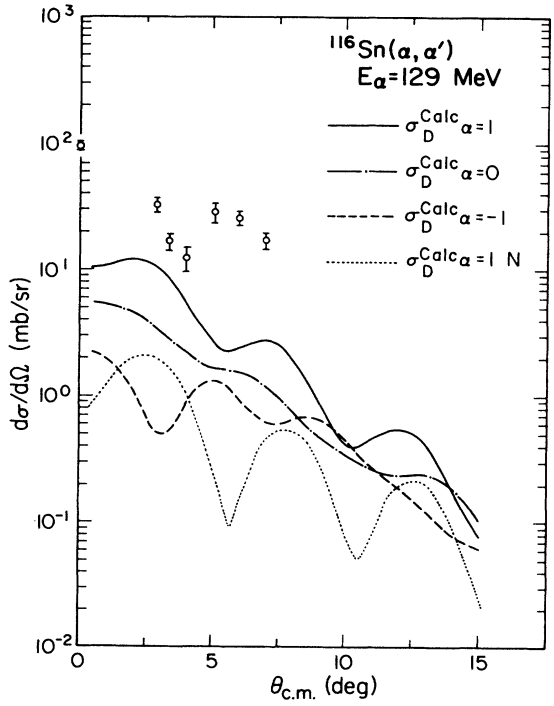

FIG. 2. Same as Fig. 1 for ^{116}Sn(α,α') with $E_\alpha=129$ MeV. The data are for the GMR with $E_x=15.6$ MeV, taken from Ref. 2.

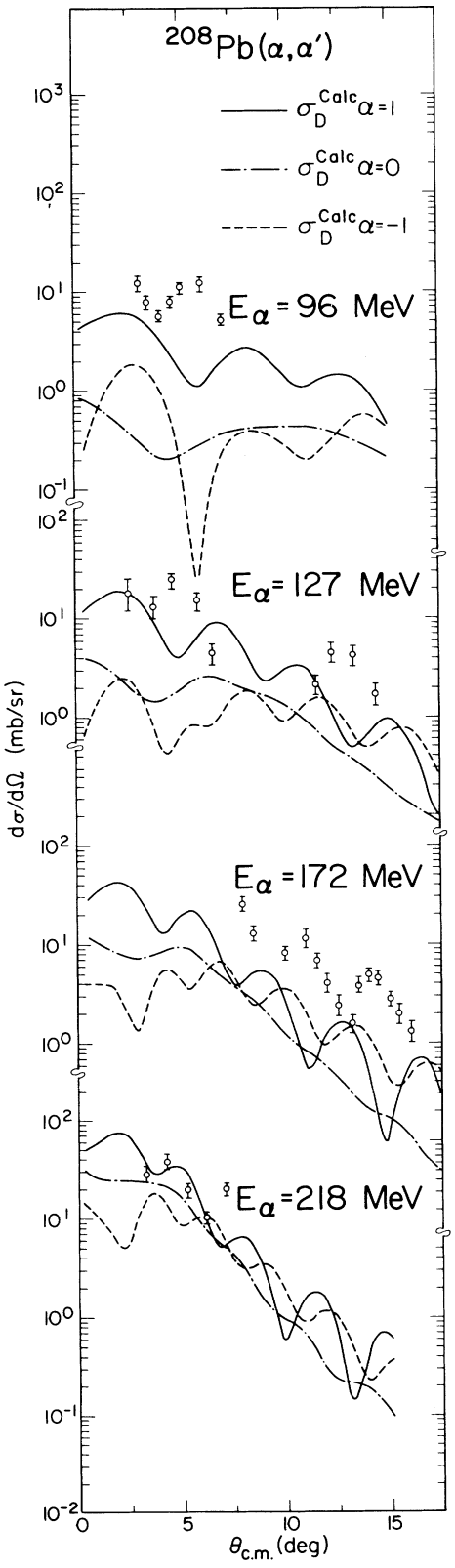

FIG. 3. Same as Fig. 1 for ^{208}Pb(α,α') for various projectile energies. The corresponding data are for the GMR with $E_x = 13.7$ MeV, taken from Refs. 1, 3, and 4.

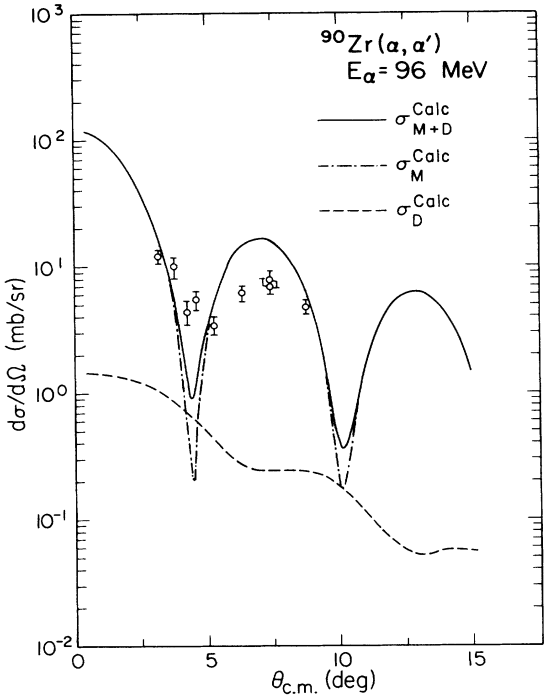

FIG. 4. Calculated, with 100% of the corresponding energy weighted sum rule, and experimental GMR cross section for the ^{90}Zr(α,α') with $E_\alpha = 96$ MeV. The dashed-dotted curve is for the GMR with $E_x = 16.2$ MeV, and the dashed curve is for the GDR with constructive Coulomb interference and $\alpha = 0.5$. Their sum, the solid curve, agrees nicely with the data, taken from Ref. 2.

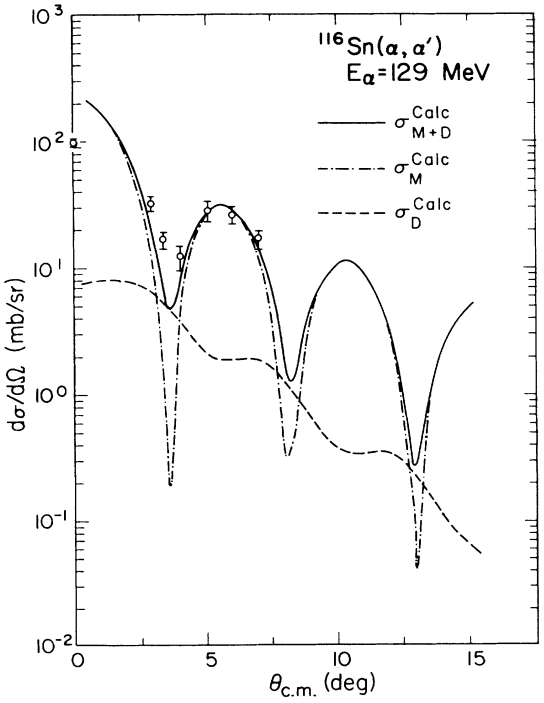

FIG. 5. Same as Fig. 4 for ^{116}Sn(α,α') with $E_\alpha = 129$ MeV. The data are for the GMR with $E_x = 15.6$ MeV, taken from Ref. 2.

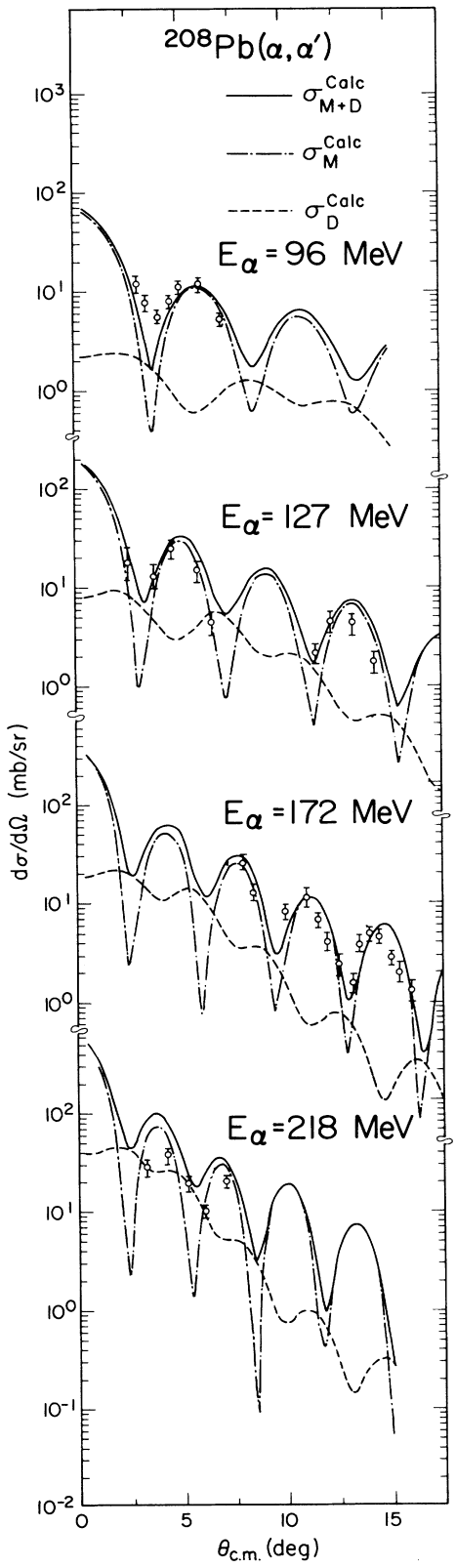

FIG. 6. Same as Fig. 4 for ^{208}Pb(α,α') for various projectile energies. The corresponding data are for the GMR with $E_x = 13.7$ MeV, taken from Refs. 1, 3, and 4.

In Figs. 4–6, we present $\sigma_D^{\rm calc}$ with $\alpha = 0.5$. There, we also presented $\sigma_M^{\rm calc}$, the GMR cross section (assuming 100% of the energy weighted sum rule strength). In these figures, we further present the sum $\sigma_{M+D}^{\rm calc} = \sigma_M^{\rm calc} + \sigma_D^{\rm calc}$. As seen, $\sigma_D^{\rm calc}$ with $\alpha = 0.5$ is generally much smaller than is $\sigma^{\rm expt}$, and thus we have $\sigma_{M+D} \simeq \sigma_M$. Noting that $\sigma_D^{\rm calc}$ given in Figs. 4–6 uses the highest plausible α value and, hence, is an upper limit, we may conclude that the contributions from the GDR are indeed small and thus can be neglected, at least for the energies in the present study below 218 MeV. We note, however, that the contributions are not completely negligible for higher E_α. The effects may become more marked if a higher E_α is used.

It is apparent in Figs. 4–6 that the data are fit rather nicely by the σ_{M+D} ($\simeq\sigma_M$), both in magnitude and angular distribution. We thus reconfirm our previous conclusion that these (α,α') data represent excitation of the GMR, rather than the GDR. We point out that our calculations do not take into account the finite solid angle of the detector system. It is clear from Figs. 4–6 that the fit to the data would be even better if the effect of angular averaging were included.

IV. FINAL REMARKS

Coupled-channel calculations of GDR cross sections were performed including both nuclear and Coulomb excitations. The results showed that in the energy range considered ($E_\alpha = 96$–218 MeV), the GDR cross sections are not very important, even when the upper limit of $\alpha = 0.5$ was used, and can rather safely be ignored in extracting the monopole strengths. The calculated GDR cross sections increase with increasing E_α, however. Therefore, at very high energies, its effect may not be negligible.

The above conclusion, which is consistent with those of Refs. 1 and 5, contradicts that drawn by Peterson.[6] To pin down the precise origin of these differences is not possible because Peterson[6] has not given the detailed form of the coupling potential he used, such as those we gave in (26), along with (14), (19), (24), and (25). Nevertheless, from what is included in Ref. 6, we point out the following features of Peterson's calculation which may lead to these differences. We first note that his simple model *ansatz* of a superposition of two diffractive patterns, associated with the different radii of the proton and neutron density distributions, is not valid. Due to the strong absorption of the α-particle (at the surface) one expects only one ($L = 1$) pattern which is associated with $R_{\rm n}$. Therefore, we consider in the following his DWBA calculation. In doing this, we refer to the revised Figs. 1 and 2 of Peterson's work appearing in his errata.[6]

(i) The transition density $\rho_{\rm tr}(\mathbf{r})$ should conserve the (a) particle number, $\int \rho_{\rm tr}(\mathbf{r}) d\mathbf{r} = 0$, and (b) center of mass, $\int \rho_{\rm tr}(\mathbf{r}) \mathbf{r}\, d\mathbf{r} = 0$. Due to the angular dependence (Y_{1M}), the corresponding transition potential fulfills requirement (a). By consistency, the corresponding transition potential should fulfill requirement (b). Peterson's *ansatz*

$$\Delta U_N = \beta \left[-\frac{N}{A} R_p \frac{\partial U_0}{\partial r_p} + \frac{Z}{A} R_n \frac{\partial U_0}{\partial r_n} \right] \quad (31)$$

for the nuclear coupling potential to the GDR violates, in general, the condition that the center of mass position should be preserved. His coupling potential [our Eq. (31)] satisfies this condition only when

$$\Delta R = R_n - R_p = \frac{1}{2} \frac{N-Z}{A} R_0 ,$$

i.e., when $\alpha = \frac{3}{4}$ (a value much larger than can be justified experimentally). For $\Delta R = 0$, the coupling potential should vanish, but his, in fact, does not.

(ii) The relative sign between the nuclear and the Coulomb coupling potentials shown in Peterson's Fig. 2 for the GDR produces a *destructive* interference. (It should be constructive.) It is seen from our calculations with $\alpha = -1.0$ that in this case the oscillations of the angular distribution are in phase with the data.

(iii) It is possible that the agreement between the data for ^{116}Sn and the solid curve of Fig. 1(a) of Peterson's work[6] is due to a too large nuclear coupling potential with a *destructive* interference. The nuclear form factor with the value of $\Delta R = 0.49$ fm used in Peterson's calculation of Fig. 1(a) does not violate the conservation of the center of mass. It corresponds to the form factor of Eq. (19) with $\alpha = \frac{3}{4}$. However, the value of β used by Peterson is much larger than that given by the Goldhaber-Teller model [see Eqs. (19), (23), and (24)]. It produces an order of magnitude enhancement in the cross section in his calculation. With such a strong nuclear coupling potential, along with a *destructive* interference, it is possible to fit the data. We also add that if one adopts the Jensen-Steinwedel model[11] for the GDR, one obtains no nuclear coupling potential for the α-particle probe.

(iv) Peterson's[6] Fig. 1(b) shows calculation for $\Delta R = 0$ which violates the conservation of the center of mass. The nuclear excitation (which should, in fact, vanish) interferes constructively with the Coulomb excitation. This interference and the too large β explain the large calculated cross section with out of phase oscillations.

In summary we conclude that according to the calculations presented in this work, the α-particle excitation of the GDR is rather small compared to the excitation of the GMR (in the energy region considered) and can be safely neglected in determining the strength of the giant monopole resonance.

The work was supported in part by the U.S. Department of Energy and the Robert A. Welch Foundation.

[1]D. H. Youngblood, C. M. Rozsa, J. M. Moss, D. R. Brown, and J. D. Bronson, Phys. Rev. Lett. **39**, 1188 (1977).
[2]C. M. Rozsa, D. H. Youngblood, J. D. Bronson, Y.-W. Lui, and U. Garg, Phys. Rev. C **21**, 1252 (1980).
[3]D. H. Youngblood, P. Bogucki, J. D. Bronson, U. Garg, Y.-W. Lui, and C. M. Rozsa, Phys. Rev. C **23**, 1997 (1981).
[4]C. Djalali, N. Marty, M. Morlet, A. Willis, V. Comparat, and R. Frascaria, Z. Phys. A **298**, 79 (1980); P. Decowski and H. P. Morsch, Nucl. Phys. **A377**, 261 (1982).
[5]T. Izumoto, Y.-W. Lui, D. H. Youngblood, T. Udagawa, and T. Tamura, Phys. Rev. C **24**, 2179 (1981).
[6]R. J. Peterson, Phys. Rev. Lett. **57**, 1550 (1986); **57**, 2771 (1986).
[7]S. Shlomo, D. H. Youngblood, T. Udagawa, and T. Tamura, Phys. Rev. Lett. (in press).
[8]B. T. Kim, T. Udagawa, D. H. Feng, and T. Tamura, University of Texas Technical Report No. UTNT-1 (unpublished).
[9]T. Tamura, Rev. Mod. Phys. **37**, 679 (1965); Oak Ridge National Laboratory Report ORNL-4152, 1967.
[10]K. Alder and H. C. A. Pauli, Nucl. Phys. **A128**, 193 (1969).
[11]G. R. Satchler, Nucl. Phys. **A195**, 1 (1972); **A224**, 596 (1974).
[12]A. Chaumeaux, V. Layly, and R. Schaeffer, Phys. Lett. **72B**, 33 (1977); L. Ray and G. W. Hoffmann, Phys. Rev. C **31**, 538 (1985).
[13]J. L. Ullmann, J. J. Kraushaar, T. G. Masterson, R. J. Peterson, R. S. Raymond, R. A. Ristinen, N. S. P. King, R. L. Boudrie, C. L. Morris, R. E. Anderson, and E. R. Siciliano, Phys. Rev. C **33**, 177 (1985).
[14]J. Decharge and D. Gogny, Phys. Rev. C **21**, 1568 (1980); J. Decharge, M. Girod, D. Gogny, and B. Grammaticos, Nucl. Phys. **A358**, 203c (1981).
[15]G. R. Satchler, *Direct Nuclear Reactions* (Oxford University Press, Oxford, 1984).
[16]S. Shlomo and G. F. Bertsch, Nucl. Phys. **A243**, 507 (1975).
[17]R. J. Peterson and R. DeHaro, Nucl. Phys. **A459**, 445 (1986).